Original Research Article

First-Principles Calculation of Optoelectronic properties of Antimony Sulfides thin film

Abstract

Antimony sulfide (Sb_2S_3) thin film have received great interests as an absorbing layer for solar cell technology. Electronic and optical properties of Sb_2S_3 thin films were studied by first principles approach. Highly accurate full-potential linearized augmented plane wave (FP-LAPW) method within density functional theory (DFT) as implemented in WIEN2k package. The simulated film is in the [001] direction using supercell method with a vacuum along z-direction so that slab and periodic images can be treated independently. The calculated values of indirect band gaps of Sb_2S_3 for various slabs were found to be 0.568, 0.596 and 0.609 eV for 1, 2 and 4 slabs respectively. This trend is consistent with the experimental work where the band gap reduced when the thickness increased. Optical properties comprising of real and imaginary parts of complex dielectric function, absorption coefficient, refractive index was also investigated to understand the optical behavior of Sb_2S_3 thin films. From analysis of optical properties, it is clearly shown that Sb_2S_3 thin films have good optical absorption in the visible light and ultraviolet wavelengths, it is anticipated that these films can be used as an absorbing layer for solar cell and optoelectronic devices

Keywords: DFT, LAPW, Sb_2S_3 thin film, Solar cell, optical properties

1 Introduction

The worldwide demand of high performance and low-cost photovoltaic devices is becoming more eminent due to extensive usage of electricity-consuming devise as a results of rapid growth of population [1, 2]. The dire requirement for low-cost and efficient optoelectronic device has led to the increase focus on a range of different source materials along with the development of method to characterize these materials [3]. CdTe and Cu(In,Ga)(S,Se) (CIGS) with 30% solar conversion efficiency are leading candidates for light-absorbing materials used in thin-film photovoltaics [4-6]. Nevertheless, the toxicity and the restrictions on the heavy metal usage for Cd and limited supply of In and Te urge for development of other alternative absorber material for large-area manufacturing compatibility [7-10]. Nowadays, the main focus of the photovoltaic community is to reduce the $\$W^{-1}$ using low-cost materials. To this point, Sb_2S_3 semiconductor material has received great attention as a promising candidate for photovoltaic applications, owing to its excellent electronic and optical properties, environmentally friendly constituent and earth-abundant, stable and simple phase with low melting point [2, 11, 12]. These optoelectronic properties make Sb_2S_3 suitable for solar cell application [13]. Sb_2S_3 is a layered semiconducting material with orthorhombic crystal structure containing 20 atoms per unit cell [14]. Sb_2S_3 is usually used as an absorbing layer in solar cells application and its performance is related to its optical properties [15, 16]. The reported absorption coefficient and optical band gap of Sb_2S_3 thin films is in the range of $10^4 - 10^4$ cm^{-1} and $1.6 - 1.8$ eV [17, 18]. Conversely, physical properties of thin film exhibits strong dependence on the thickness of the film due to quantum confinement effect or quantum size effects [19, 20]. Therefore, researchers have studied thin film of Sb_2S_3 intensively to evaluate its physical properties. It has been established that stable Sb_2S_3 thin film possess an orthorhombic crystal structure [21, 22] with direct band-gap energy of 1.5–2.4 eV [23-25].

Tuning the thickness in semiconductors thin films can lead to the change in their electronic and optical properties not exhibited by their bulk counterpart, due to the confinement of the movement of electrons [26]. Recent study on Sb_2S_3 thin film showed that the increase in thickness from 77 to 206 nm lead to the decrease in the bandgap energy, indicating existence of quantum size effect [27]. It is well known that electronic and optical properties of semiconductor materials play an important role in determining their optoelectronics properties [28]. Density functional theory (DFT) based on GGA and LDA has been used for investigating electronic and optical properties of semiconductor materials [29, 30] particularly thin film structure, since GW method is prohibitively expensive and impractical for thin films calculations of semiconductors [31-33] . First principles calculation means an approach of doing calculations that rely on a well-established and fundamental laws of science that does not involve any fitting techniques, special models or suppositions. Several theoretical works on thin film studying the effect of thickness on the solid properties has been done [34-38]. Although extensive studies on Sb_2S_3 bulk using DFT have been done [14, 39-43]. To the best of our knowledge investigation of electronic and optical properties with highly accurate all-electron full potential linearized augmented plane wave (FP-LAPW) on Sb_2S_3 thin film with different thickness have not been explored yet, due to its complex and disordered structure. In this paper, electronic and optical properties of Sb_2S_3 (0 0 1) thin film with different thickness were calculated within Engel Vosko generalized gradient approximation (EV-GGA) [44].

2 Computational Details

Electronic and optical properties of Sb_2S_3 thin films with different thickness are performed via first-principles full-potential linearized augmented-plane-wave (FP-LAPW) method within the DFT scheme as employed in WIEN2k program [45]. Under slab geometry supercell, the thin films are formed by using optimized lattice constants in (001) direction using (1×1) cell for various thickness (1–8 slabs). A slab is represented by optimized bulk of orthorhombic Sb_2S_3 (α=β= γ=90°, a= 1.1646 nm, b= 0.3953 nm and c= 1.1587 nm) As illustrated in Figure 2**.** A large vacuum of 3 nm along z-plane was considered to avoid inter-layer interaction. Table 1 show a list of thicknesses for different number of layers (from 1–8 slabs) for Sb_2S_3 (0 0 1) thin films. To calculate the total energy of the system, EV-GGA approximation were used as the exchange potentials. The EV-GGA potential has been justified to provide quite accurate band gaps for various semiconducting materials including Sb_2S_3 [39, 41]. The wave functions are expanded in spherical harmonics inside the Muffin-Tin radius (R_{MT}) around each nucleus [46]. To ensure the accuracy of the calculation, the R_{MT} are used for both Sb and S atoms and $R_{MT}K_{max}$ was set to be -7 Ry. Other perimeters included in the calculation are $G_{max} = 7$ and $I_{max} = 12$. Where Gmax is the maximum expansion magnitude of the basis function and I_{max} is the maximum expansion magnitude of the wavefunctions in spherical harmonics inside the muffin tins (MTs). These parameters are selected to determine the extent of the matrix. Three hundred k-points in the first Brillouin zone were adopted in the calculations (250 points in the irreducible part of the surface Brillouin zone). The iteration was halted when the difference total energy was less than 0.00001 Ry between steps, taken as a convergence criterion.

Table 1. Thicknesses for different number of layers (from 1–8 slabs) for Sb_2S_3 (0 0 1) thin films.

Number of slabs	thickness(nm)
1	1.16
2	2.31
4	4.63
6	6.95
8	9.27

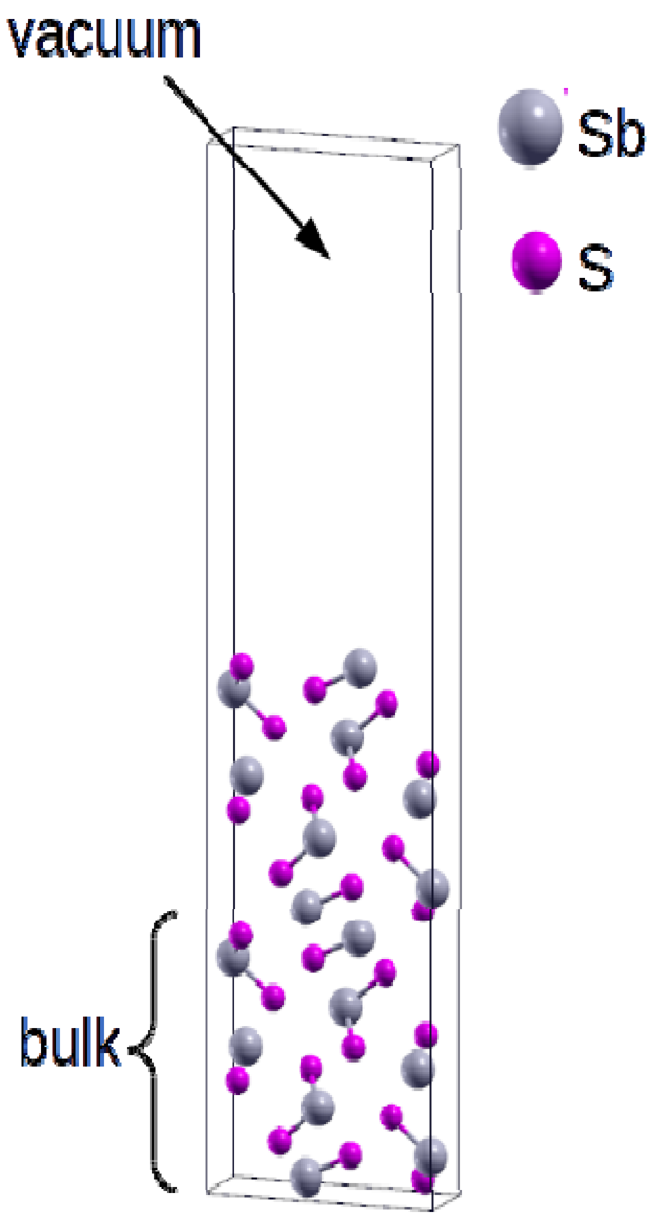

Figure 1: Crystal structure of 2 slab of Sb_2S_3 (001) film with 3nm vacuum

3 Results and Discussion

3.1 Electronic Structure

The electronic properties in concern are band structures and density of states (DOS). For better understanding of the thickness dependence on electronic band structure, we analyze the electronic band structure of Sb_2S_3 (001) film with respect to the number of slabs. The k path selected along high symmetry point in the first Brillouin zone is $Y \rightarrow \Gamma \rightarrow S \rightarrow \Gamma$. The band structure plots of Sb_2S_3 in bulk form and film from 1 to 8 slabs with EV-GGA along selected high symmetry directions in the Brillouin zone are presented in Figure 2. The Fermi energy at the bottom of conduction band is defined to be zero energy (0 eV). EV-GGA functionals is selected in our calculations, it provides good predictions on band gap value for both bulk and surface states of numerous semiconductor materials than bare GGA [47-49]. Lack of study on 2D materials using this exchange-correlation functional motivated us to use it in our present calculations. It is evident from Figure 2 that Sb_2S_3 slabs exhibits indirect band gap with valence band maximum lying between S and Γ and conduction band minimum at Γ-symmetry point respectively. The indirect band gap value of bulk Sb_2S_3 with EV-GGA functionals without spin-orbit coupling was found to be 1.661 eV and this value is in good agreement with previous theoretical work and experimental measurement of 1.1-2.8 eV [13, 14, 50]. The calculated values of indirect energy gaps of Sb_2S_3 slabs was found to be 0.568 and 0.596 eV for slab 1 and 2 respectively and this trend is consistent with the experimental work where the band gap value reduced when the thickness increased [27]. This change of band gap becomes evident that thickness of films has effect in material physical properties. On the other hand, the magnitude of the energy band gap remains the same when the films thickness is more than 3 slabs. Although the energy band gap values are the same when the film thickness is more than 3 slabs but the number of bands in both conduction and valence band enhanced as the thickness of Sb_2S_3 (001) films increases and this trend is in quite agreement with previous thin film studies. It is clear from Figure 2 that the indirect energy gap of Sb_2S_3 slabs reduced by 1 eV with respect to its bulk counterpart. The reason for low band gap in Sb_2S_3 films when compared with the bulk form is due to quantum confinement effect that had been discussed and confirmed in various surface studies [51-54]. To further probe the nature of the energy gap, we have also study the total density of state (DOS) of Sb_2S_3 films with different slabs within EV-GGA. Figure 3 shows the graph of total DOS. From the total DOS plots, the peaks of the state density in the valence band region increases significantly near the Fermi level with the number while in the conduction band region the increase start at 1.5 eV. The increment in total DOS is correspond to the increase in number of atoms and electrons in the films. Therefore, it is possible to exploit the quantum confinement effect to tune the electronic properties in Sb_2S_3 films.

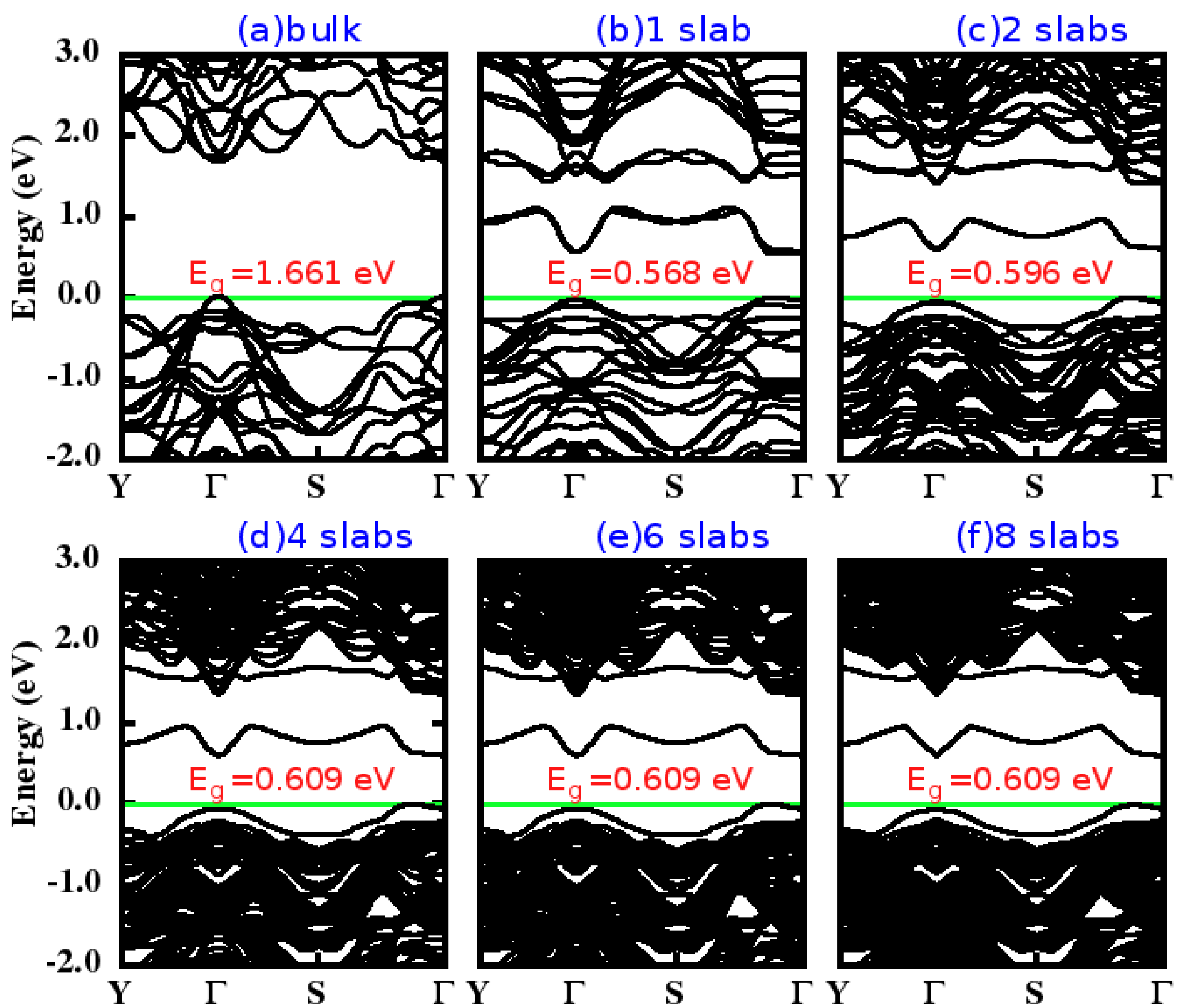

Figure 2. Band structures of the bulk Sb_2S_3 (a) and Sb_2S_3 nanofilms with five different thicknesses: 1 slab (b), 2 slabs (c), 3 slabs (d), 4 slabs (e), 5 slabs(f).

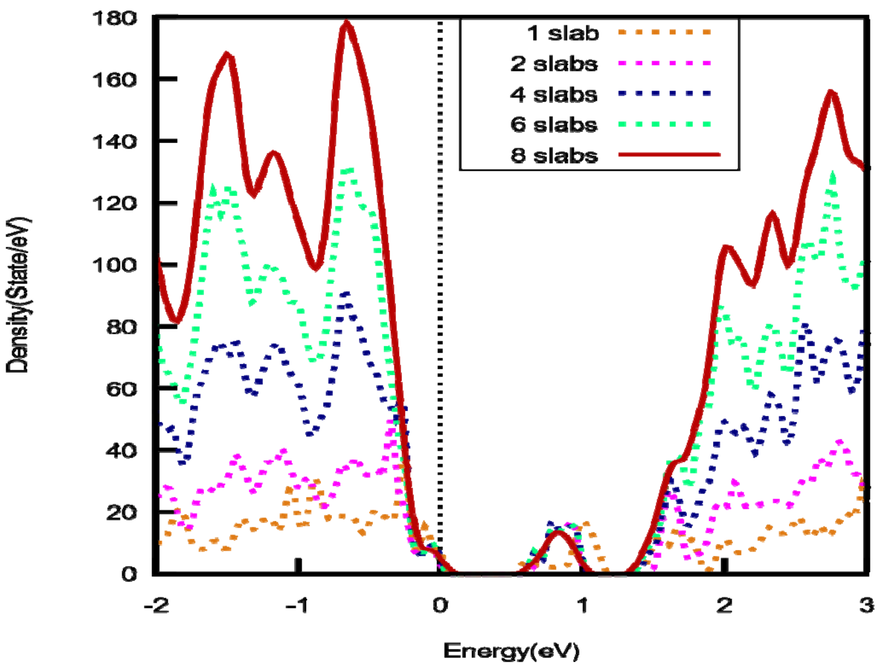

Figure 3: Total density of states of the Sb_2S_3 nanofilms with various thickness

3.3 Optical properties

This part provides several optical parameters of Sb_2S_3 thin films which examined for the first time by highly accurate first principles all electron full potential linearized augmented plane wave method. Optical parameters of material normally explain the behavior of the material when exposed to the electromagnetic radiation and they also help in predicting band structure configuration. Understanding optical behavior of material is essential to estimate its usefulness and applicability for optoelectronic application [55]. Optical behavior is strongly associated with electronic structure [28]. As observed in the electronic band structure analysis, the geometry of the electronic structure for Sb_2S_3 thin film changed with films thickness. Several experimental studies have showed that optical properties of Sb_2S_3 thin film dependent on the thickness of the film. However, to the best of our knowledge theoretical investigation on Sb_2S_3 thin films have not been reported yet on optical properties. In order to describe the said parameters quantitively, it is essential to evaluate dielectric function. Dielectric function is the ratio of the permittivity of a material to the permittivity of free space, whereas permittivity is the measure of the resistance of a material when an electric field is induced in a material. All the dielectric materials are insulator but all the insulators are not dielectric [56]. The dielectric function consists of real ($\varepsilon_1(\omega)$) and imaginary part ($\varepsilon_2(\omega)$). It is represented as follows:

$$\varepsilon(\omega) = \varepsilon_1(\omega) + i\varepsilon_2(\omega) \qquad (1)$$

Where $\varepsilon_1(\omega)$ is real part and $\varepsilon_2(\omega)$ is imaginary part of the dielectric function. Physical properties and band structure rely strongly on $\varepsilon(\omega)$.

As mentioned, we analyzed the optical properties based on EV-GGA functionals. From the knowledge of electronic band structure of a solid, the imaginary part of the dielectric function, $\varepsilon_2(\omega)$ can be calculated from Kubo–Greenwood equation as show in Equation 2:

$$\varepsilon_2(\omega) = \frac{2\pi e^2}{\Omega\varepsilon_0} |\langle\psi_k^c|\hat{u}\times\vec{r}|\psi_k^v\rangle|\delta\left(E_k^c - (E_k^v + E)\right) \qquad (2)$$

Once we know the imaginary part, the real part, $\varepsilon_1(\omega)$ can be obtain from the Kramers–Kronig relations in Equation 3.

Real part of dielectric function gives information about the refractive index of any material under investigation while imaginary part explains the absorption of light. The calculated imaginary (ε_2) and the real (ε_1) parts of the dielectric functions as a function of the photon energy are shown in Figure 4(a)-(b) in the region of 0-20 eV. It has been established that Sb_2S_3 semiconductor has orthorhombic symmetry. This symmetry has three independent components of dielectric function but for this work, we only consider polarization along [001] direction.

$$\varepsilon_1(\omega) = 1 + \left(\frac{2}{\pi}\right)\int_0^\infty d\omega' \frac{\omega'^2\varepsilon_2(\omega')}{\omega'^2-\omega^2} \qquad (3)$$

The static dielectric constant, $\varepsilon_1(0)$ is the real part of dielectric constant at zero energy. These parameters were analyzed for Sb_2S_3 thin films as can be seen in Figure 4(a). Table 3 show an illustration of the static dielectric constant for different slabs. From the results, it is noticed that the value of static dielectric constant increases as the thin films thickness increases. Conversely, these values are important parameters that could be also used to obtain the energy band gap values of Sb_2S_3 thin films by via Penn Model relation $\varepsilon_1(0) \approx \left(\hbar\omega_p / E_g\right)^2 + 1$ [57]. Using plasma energy $\hbar\omega_p$ and the value of $\varepsilon_1(0)$, the value of energy gap of the title material can be calculated by using Penn expression. Interestingly, it was also observed that Sb_2S_3 thin films possess plasmonic behavior when the thickness of the film is greater than one slab (1 slab). This negative behavior of real part (plasmonic behavior) is another exciting feature to make Sb_2S_3 thin film suitable for many applications [58-60].

It has been established that imaginary part of dielectric function is directly connected with the energy band structure. The edge of optical absorption (first critical point) occurs at about 0.562, 0.589, 0.608, 0.607, 0.606 eV for 1, 2, 4, 6 and 8 slabs. Hence, the calculated imaginary part of dielectric function shows that the first critical point peak is related to the transition from the valence to the conduction band states corresponded to the fundamental band gap. The results of imaginary part of dielectric function indicated that Sb_2S_3 thin films has strong absorption behavior in the visible light frequency, which depicts its suitability for solar cell applications. Apparently, due to crystallinity of the films, the optical absorption increases with the increase in the film thickness.

Table 3: Static dielectric, $\varepsilon_1(0)$ and Static refractive index, n(0) of Sb2S3(001) thin films for different slabs.

		Static dielectric, $\varepsilon_1(0)$	Static refractive index, n(0)
Number of slab	1	3.75	1.94
	2	5.80	2.41
	4	7.82	2.80
	6	8.83	2.97
	8	9.59	3.10
Bulk		12.7	3.57

$$\alpha(\omega) = \frac{\omega}{c}\sqrt{2\left(\sqrt{\varepsilon_1^2(\omega) + \varepsilon_2^2(\omega)} - \varepsilon_1(\omega)\right)} \quad (3)$$

$$n(\omega) = \sqrt{\left(\frac{\sqrt{\varepsilon_1^2(\omega) + \varepsilon_2^2(\omega)} + \varepsilon_1(\omega)}{2}\right)} \quad (4)$$

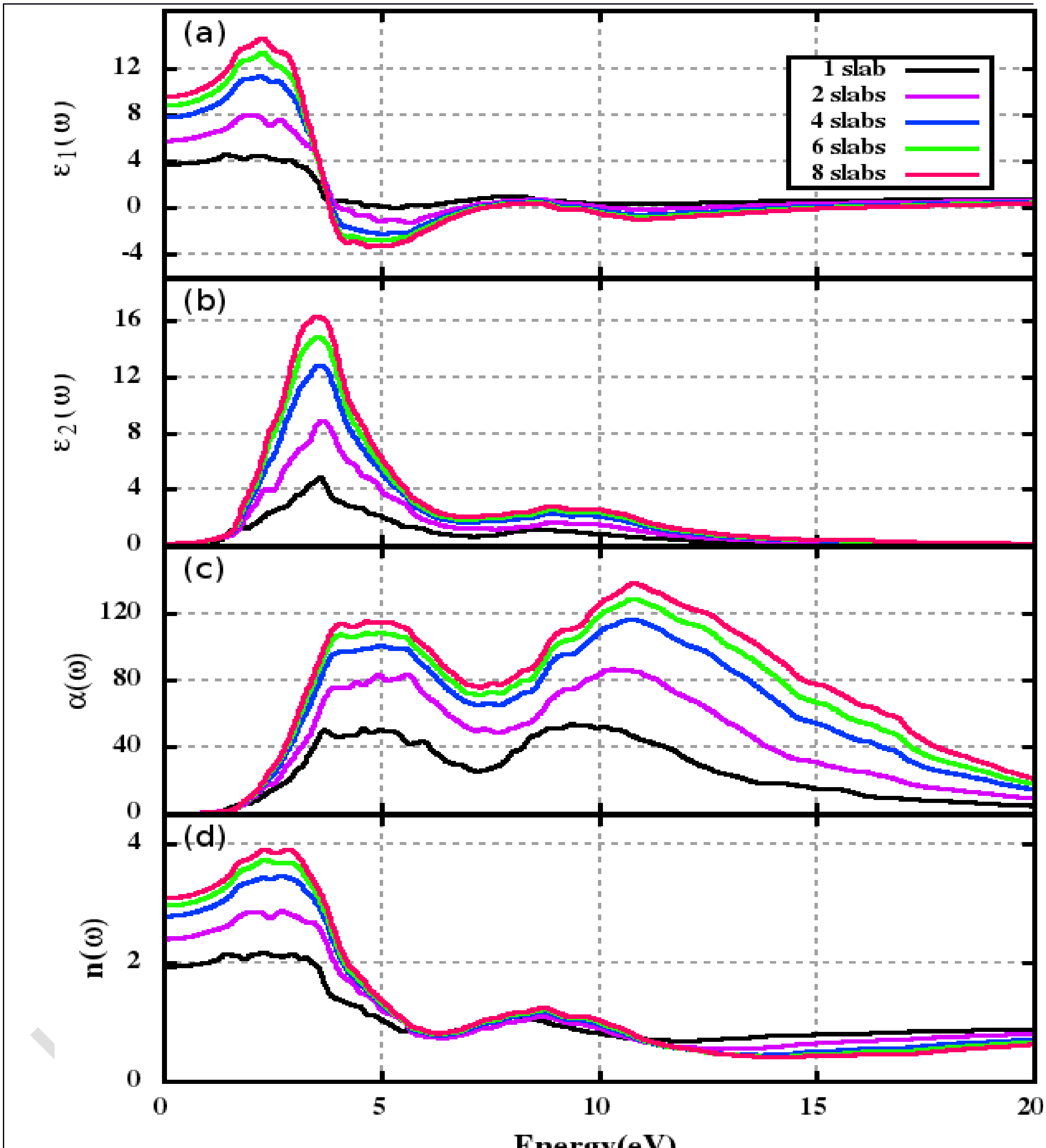

Figure 4 (a) Real and (b) imaginary part of dielectric functions, (c)absorption coefficient and (d)refractive index for different slabs of Sb_2S_3 (001) film shown.

Using the knowledge of the complex dielectric constant, other optical parameters such as absorption coefficient, α(ω) and refractive index, n(ω) can be determined. Figure 4 (c)-(d) show the energy dependence of absorption coefficient and refractive index. For photovoltaic applications it is important to use a material with a suitable band gap having large absorption coefficient [61]. When light rays strike the surface of a material, some part of its energy is reflected while some are transferred to the surface of the material. This transfer of energy to the surface is called Absorption of light and It is represented in term of absorption coefficient α(ω). Graph of absorption coefficient as a function of photon energy is presented in Figure 4(c). From this graph, it is clearly that Sb_2S_3 thin films have good absorption coefficient in the visible light and ultraviolet wavelengths. Since Sb_2S_3 thin films show good absorption coefficient in the visible light and ultraviolet wavelengths for all thickness, it is anticipated that these films can be used as an absorbing layer for solar cell and optoelectronic devices. The curves of refractive index n(ω) in Figure 4 (d) are similar to the real part of dielectric function $\varepsilon_1(\omega)$ which is in accordance with the established theory [62]. The values of static refraction index for different thickness of Sb_2S_3 (001) thin film are given in Table 3**.** From the graph, we observed that the values of n(ω) in Sb_2S_3 (001) thin films are influenced by film thickness.

4 Conclusion

In summary, Electronic and optical properties of Sb_2S_3 thin films were studied by highly accurate full-potential linearized augmented plane wave (FP-LAPW) approach based on DFT within EV-GGA exchange-correlation. The calculated values of indirect band gaps of Sb_2S_3 for various slabs were found to be 0.568, 0.596 and 0.609 eV for 1, 2 and 4 slabs respectively. This trend is in good agreement with experimental work where the band gap reduced when the thickness increased. Optical properties including real and imaginary parts of complex dielectric function, absorption coefficient, refractive index was also investigated to understand the optical behavior of Sb_2S_3 thin films. From the analysis of optical properties, it was clearly shown that Sb_2S_3 thin films have good optical absorption in the visible light and ultraviolet wavelengths, it is therefore, anticipated that these films can be used as an absorbing layer for solar cell and other optoelectronic devices.

REFERENCES

[1] N. Ali, A. Hussain, R. Ahmed, W.W. Shamsuri, A. Shaari, N. Ahmad, S. Abbas, Antimony sulphide, an absorber layer for solar cell application, Applied Physics A, 122 (2016) 23.

[2] C. Gao, J. Huang, H. Li, K. Sun, Y. Lai, M. Jia, L. Jiang, F. Liu, Fabrication of Sb2S3 thin films by sputtering and post-annealing for solar cells, Ceramics International, (2018).

[3] A. LAWAL, THEORETICAL STUDY OF STRUCTURAL, ELECTRONIC AND OPTICAL PROPERTIES OF BISMUTH-SELENIDE, BISMUTH-TELLURIDE AND ANTIMONY-TELLURIDE/GRAPHENE HETEROSTRUCTURE FOR BROADBAND PHOTODETECTOR, in, Universiti Teknologi Malaysia, 2017.

[4] K. Sasihithlu, N. Dahan, J.-J. Greffet, Light Trapping in Ultrathin CIGS Solar Cell With Absorber Thickness of 0.1$\mu $ m, IEEE Journal of Photovoltaics, 8 (2018) 621-625.

[5] R.M. Geisthardt, M. Topič, J.R. Sites, Status and potential of CdTe solar-cell efficiency, IEEE Journal of photovoltaics, 5 (2015) 1217-1221.

[6] A. Romeo, M. Terheggen, D. Abou□Ras, D. Bätzner, F.J. Haug, M. Kälin, D. Rudmann, A. Tiwari, Development of thin□film Cu (In, Ga) Se2 and CdTe solar cells, Progress in Photovoltaics: Research and Applications, 12 (2004) 93-111.

[7] T.D. Lee, A.U. Ebong, A review of thin film solar cell technologies and challenges, Renewable and Sustainable Energy Reviews, 70 (2017) 1286-1297.

[8] C. Wadia, A.P. Alivisatos, D.M. Kammen, Materials availability expands the opportunity for large-scale photovoltaics deployment, Environmental science & technology, 43 (2009) 2072-2077.

[9] V. Fthenakis, Sustainability of photovoltaics: The case for thin-film solar cells, Renewable and Sustainable Energy Reviews, 13 (2009) 2746-2750.

[10] C. Candelise, J.F. Speirs, R.J. Gross, Materials availability for thin film (TF) PV technologies development: a real concern?, Renewable and Sustainable Energy Reviews, 15 (2011) 4972-4981.

[11] I. Efthimiopoulos, C. Buchan, Y. Wang, Structural properties of Sb 2 S 3 under pressure: evidence of an electronic topological transition, Scientific reports, 6 (2016) 24246.

[12] L. Zheng, K. Jiang, J. Huang, Y. Zhang, B. Bao, X. Zhou, H. Wang, B. Guan, L.M. Yang, Y. Song, Solid-state nanocrystalline solar cells with an antimony sulfide absorber deposited by an in situ solid–gas reaction, Journal of Materials Chemistry A, 5 (2017) 4791-4796.

[13] A. Radzwan, R. Ahmed, A. Shaari, Y.X. Ng, A. Lawal, First-principles calculations of the stibnite at the level of modified Becke–Johnson exchange potential, Chinese Journal of Physics, 56 (2018) 1331-1344.

[14] H. Koc, A.M. Mamedov, E. Deligoz, H. Ozisik, First principles prediction of the elastic, electronic, and optical properties of Sb2S3 and Sb2Se3 compounds, Solid State Sciences, 14 (2012) 1211-1220.

[15] P. Nair, R. González-Lua, M.C. Rodríguez, J.C. Martínez, O. GomezDaza, M.S. Nair, Antimony sulfide absorbers in solar cells, ECS Transactions, 41 (2011) 149-156.

[16] S. Ito, K. Tsujimoto, D.-C. Nguyen, K. Manabe, H. Nishino, Doping effects in Sb2S3 absorber for full-inorganic printed solar cells with 5.7% conversion efficiency, International Journal of Hydrogen Energy, 38 (2013) 16749-16754.

[17] M. Kriisa, M. Krunks, I.O. Acik, E. Kärber, V. Mikli, The effect of tartaric acid in the deposition of Sb2S3 films by chemical spray pyrolysis, Materials Science in Semiconductor Processing, 40 (2015) 867-872.

[18] Y.C. Choi, D.U. Lee, J.H. Noh, E.K. Kim, S.I. Seok, Highly improved Sb2S3 sensitized□inorganic–organic heterojunction solar cells and quantification of traps by deep□level transient spectroscopy, Advanced Functional Materials, 24 (2014) 3587-3592.

[19] D. Jena, A. Konar, Enhancement of carrier mobility in semiconductor nanostructures by dielectric engineering, Physical review letters, 98 (2007) 136805.
[20] G.B. Bhandari, K. Subedi, Y. He, Z. Jiang, M. Leopold, N. Reilly, H.P. Lu, A.T. Zayak, L. Sun, Thickness-controlled synthesis of colloidal PbS nanosheets and their thickness-dependent energy gaps, Chemistry of Materials, 26 (2014) 5433-5436.
[21] P. Chate, D. Sathe, S. Lakde, V. Bhabad, A novel method for the deposition of polycrystalline Sb 2 S 3 thin films, Journal of Materials Science: Materials in Electronics, 27 (2016) 12599-12603.
[22] S. Qiao, J. Liu, Z. Li, S. Wang, G. Fu, Sb 2 S 3 thickness-dependent lateral photovoltaic effect and time response observed in glass/FTO/CdS/Sb 2 S 3/Au structure, Optics express, 25 (2017) 19583-19594.
[23] Y.S. Lee, M. Bertoni, M.K. Chan, G. Ceder, T. Buonassisi, Earth abundant materials for high efficiency heterojunction thin film solar cells, in: Photovoltaic Specialists Conference (PVSC), 2009 34th IEEE, IEEE, 2009, pp. 002375-002377.
[24] N. Ţigaˇu, C. Gheorghieş, G. Rusu, S. Condurache-Bota, The influence of the post-deposition treatment on some physical properties of Sb2S3 thin films, Journal of non-crystalline solids, 351 (2005) 987-992.
[25] A. Salem, M.S. Selim, Structure and optical properties of chemically deposited Sb2S3 thin films, Journal of Physics D: Applied Physics, 34 (2001) 12.
[26] K.F. Mak, C. Lee, J. Hone, J. Shan, T.F. Heinz, Atomically thin MoS 2: a new direct-gap semiconductor, Physical review letters, 105 (2010) 136805.
[27] R. Mane, C. Lokhande, Thickness-dependent properties of chemically deposited Sb2S3 thin films, Materials chemistry and physics, 82 (2003) 347-354.
[28] M.L. Cohen, J.R. Chelikowsky, Electronic structure and optical properties of semiconductors, Springer Science & Business Media, 2012.
[29] L. Sham, M. Schlüter, Density-functional theory of the energy gap, Physical review letters, 51 (1983) 1888.
[30] H. Xiao, J. Tahir-Kheli, W.A. Goddard III, Accurate band gaps for semiconductors from density functional theory, The Journal of Physical Chemistry Letters, 2 (2011) 212-217.
[31] J.M. Crowley, J. Tahir-Kheli, W.A. Goddard III, Accurate Ab Initio Quantum Mechanics Simulations of Bi2Se3 and Bi2Te3 Topological Insulator Surfaces, The journal of physical chemistry letters, 6 (2015) 3792-3796.
[32] T. Demján, M. Vörös, M. Palummo, A. Gali, Electronic and optical properties of pure and modified diamondoids studied by many-body perturbation theory and time-dependent density functional theory, The Journal of chemical physics, 141 (2014) 064308.
[33] E. Baldini, L. Chiodo, A. Dominguez, M. Palummo, S. Moser, M. Yazdi-Rizi, G. Auböck, B.P. Mallett, H. Berger, A. Magrez, Strongly bound excitons in anatase TiO2 single crystals and nanoparticles, Nature Communications, 8 (2017).
[34] W. Jin, P.-C. Yeh, N. Zaki, D. Zhang, J.T. Sadowski, A. Al-Mahboob, A.M. van Der Zande, D.A. Chenet, J.I. Dadap, I.P. Herman, Direct measurement of the thickness-dependent electronic band structure of MoS 2 using angle-resolved photoemission spectroscopy, Physical review letters, 111 (2013) 106801.
[35] A. Dashora, U. Ahuja, K. Venugopalan, Electronic and optical properties of MoS2 (0 0 0 1) thin films: Feasibility for solar cells, Computational Materials Science, 69 (2013) 216-221.
[36] M. Ye, D. Winslow, D. Zhang, R. Pandey, Y. Yap, Recent advancement on the optical properties of two-dimensional molybdenum disulfide (MoS2) thin films, in: Photonics, Multidisciplinary Digital Publishing Institute, 2015, pp. 288-307.
[37] A. Kuc, N. Zibouche, T. Heine, Influence of quantum confinement on the electronic structure of the transition metal sulfide T S 2, Physical Review B, 83 (2011) 245213.
[38] L.-p. Wang, Z.-x. Zhang, C.-l. Zhang, B.-s. Xu, Effects of thickness on the structural, electronic, and optical properties of MgF2 thin films: the first-principles study, Computational Materials Science, 77 (2013) 281-285.

[39] T.B. Nasr, H. Maghraoui-Meherzi, H.B. Abdallah, R. Bennaceur, Electronic structure and optical properties of Sb2S3 crystal, Physica B: Condensed Matter, 406 (2011) 287-292.
[40] J.-h. Chen, X.-h. Long, C.-h. Zhao, D. Kang, J. Guo, DFT calculation on relaxation and electronic structure of sulfide minerals surfaces in presence of H 2 O molecule, Journal of Central South University, 21 (2014) 3945-3954.
[41] A. Radzwan, R. Ahmed, A. Shaari, A. Lawal, Y.X. Ng, First-principles calculations of antimony sulphide Sb2S3, Malaysian Journal of Fundamental and Applied Sciences, 13 (2017).
[42] T.B. Nasr, H. Maghraoui-Meherzi, N. Kamoun-Turki, First-principles study of electronic, thermoelectric and thermal properties of Sb2S3, Journal of Alloys and Compounds, 663 (2016) 123-127.
[43] M.R. Filip, C.E. Patrick, F. Giustino, G W quasiparticle band structures of stibnite, antimonselite, bismuthinite, and guanajuatite, Physical Review B, 87 (2013) 205125.
[44] E. Engel, S.H. Vosko, Exact exchange-only potentials and the virial relation as microscopic criteria for generalized gradient approximations, Physical Review B, 47 (1993) 13164.
[45] P. Blaha, K. Schwarz, G.K. Madsen, D. Kvasnicka, J. Luitz, wien2k, An augmented plane wave+ local orbitals program for calculating crystal properties, (2001).
[46] K. Schwarz, DFT calculations of solids with LAPW and WIEN2k, Journal of Solid State Chemistry, 176 (2003) 319-328.
[47] W. Khan, S. Goumri□Said, Engel–Vosko generalized gradient approximation within DFT investigations of optoelectronic and thermoelectric properties of copper thioantimonates (III) and thioarsenate (III) for solar□energy conversion, physica status solidi (b), 253 (2016) 583-590.
[48] T. Benmessabih, B. Amrani, F.E.H. Hassan, F. Hamdache, M. Zoaeter, Computational study of AgCl and AgBr semiconductors, Physica B: Condensed Matter, 392 (2007) 309-317.
[49] N. Muhammad, A. Khan, S.H. Khan, M.S. Siraj, S.S.A. Shah, G. Murtaza, Engel-Vosko GGA calculations of the structural, electronic and optical properties of LiYO2, Physica B: Condensed Matter, 521 (2017) 62-68.
[50] A. Kyono, M. Kimata, Structural variations induced by difference of the inert pair effect in the stibnite-bismuthinite solid solution series (Sb, Bi) 2S3, American Mineralogist, 89 (2004) 932-940.
[51] Z. Gan, L. Liu, H. Wu, Y. Hao, Y. Shan, X. Wu, P.K. Chu, Quantum confinement effects across two-dimensional planes in MoS2 quantum dots, Applied Physics Letters, 106 (2015) 233113.
[52] Y. Zhang, T.-R. Chang, B. Zhou, Y.-T. Cui, H. Yan, Z. Liu, F. Schmitt, J. Lee, R. Moore, Y. Chen, Direct observation of the transition from indirect to direct bandgap in atomically thin epitaxial MoSe2, Nature nanotechnology, 9 (2014) 111-115.
[53] C. Weisbuch, B. Vinter, Quantum semiconductor structures: fundamentals and applications, Elsevier, 2014.
[54] J. Dai, X.C. Zeng, Bilayer phosphorene: effect of stacking order on bandgap and its potential applications in thin-film solar cells, The journal of physical chemistry letters, 5 (2014) 1289-1293.
[55] J. Singh, Optical properties of condensed matter and applications, John Wiley & Sons, 2006.
[56] M. Subramanian, D. Li, N. Duan, B. Reisner, A. Sleight, High dielectric constant in ACu3Ti4O12 and ACu3Ti3FeO12 phases, Journal of Solid State Chemistry, 151 (2000) 323-325.
[57] D.R. Penn, Wave-number-dependent dielectric function of semiconductors, Physical Review, 128 (1962) 2093.
[58] S. Savoia, G. Castaldi, V. Galdi, A. Alù, N. Engheta, PT-symmetry-induced wave confinement and guiding in ε-near-zero metamaterials, Physical Review B, 91 (2015) 115114.
[59] Y. Li, N. Engheta, Supercoupling of surface waves with ε-near-zero metastructures, Physical Review B, 90 (2014) 201107.
[60] A. Lawal, A. Shaari, R. Ahmed, N. Jarkoni, First-principles investigations of electron-hole inclusion effects on optoelectronic properties of Bi2Te3, a topological insulator for broadband photodetector, Physica B: Condensed Matter, 520 (2017) 69-75.
[61] A. Fahrenbruch, R. Bube, Fundamentals of solar cells: photovoltaic solar energy conversion, Elsevier, 2012.
[62] M. Fox, Optical properties of solids, in, AAPT, 2002.